Supporting Information

N-7' methylation in apramycin: biosynthesis and biological role

Qian Zhang, Chang He, Jing Sun, Zixin Deng, Yi Yu*

Department of Gastroenterology, Zhongnan Hospital of Wuhan University, Hubei Clinical Center and Key Laboratory of Intestinal and Colorectal Disease, School of Pharmaceutical Sciences, Wuhan University, 185 East Lake Road, Wuhan 430071, P. R. China

* Corresponding author, Email: yu_yi@whu.edu.cn

Table of Contents

1. Supplementary Methods

Bacterial Strains and Biochemicals

E. coli strains DH10B used for cloning and BL21(DE3) used for protein overexpression were purchased from Weidi Biotechnology (Shanghai, China). *E. coli* strain ET12567/pUZ8002 was used for conjugation between *E. coli* and *S. tenebrarius.* Kanamycin, chloramphenicol, streptomycin sulfate salt, spectinomycin dihydrochloride pentahydrate, isopropyl β-D-1-thiogalactopyranoside (IPTG) and *S*-adenosyl-L-methionine (SAM) were purchased from Sigma-Aldrich (USA). Nalidixic acid were purchased from AMRESCO (USA). Enzymes were purchased from Takara Biotechnology (Dalian, China) or from Vazyme Biotech (Nanjing, China). Ni-NTA-affinity resin was purchased from GenScript (Nanjing, China). Oligonucleotides and primers were synthesized at TSINGKE Biological Technology (Wuhan, China).

Cultures and Fermentation Conditions

E. coli strains were cultivated in Luria-Bertani (LB) or LB agar medium (1%tryptone, 0.5% yeast extract,1% NaCl, 1.2% agar) at 37 °C and 220 rpm shaker. The wild type and mutant strains of *S. tenebrarius* were cultivated on SPA medium (2% soluble starch, 0.1% beef extract, 0.05% $MgSO_4$, 0.1% KNO_3, 0.05% NaCl, 0.05% K_2HPO_4, 2% agar) at 37 °C for spore production. For fermentation and detection of apramycin related compounds, seed culture was prepared in 5 mL TSBY medium (3% tryptone soya broth and 0.5% yeast extract) at 37 °C with shaking at 220 rpm for 2 d, before subcultured into 50 mL Minimal medium (0.1% $(NH4)_2SO_4$, 0.05% K_2HPO_4, 0.02% $MgSO_4{\cdot}7H_2O$, 0.001% $FeSO_4{\cdot}7H_2O$ and 1% glucose) at 37°C with shaking at 220 rpm for 3~7d.

Construction of gene knockout and complement plasmids

For *aprI* and *aprJ* inactivation, upstream fragment and downstream fragment were amplified respectively by PCR from *S. tenebrarius* genomic DNA (Table S1). Purified fragments were cloned into the *Hind*III/*EcoR*I sites of shuttle vector pWHU258[1] using Hieff Clone® Plus Multi One Step Cloning Kit (Yeasen, China). The gene (*aprI*, *aprJ, aprZ*) knockout vectors, denoted as pWHU450, pWHU340, pWHU344[2](Table S1, S2), respectively, were then transferred into *S. tenebrarius via E. coli-Streptomyces* conjugation. The resulting in-frame deletion mutants were screened and confirmed by PCR analysis and DNA sequencing (Figure S1, S7, S9, S15, S16).

The *aprI* complementation plasmid was generated by inserting *aprI* into pWHU268 between *NdeI/EcoRI* sites (Table S1, S2). The resulting plasmids pWDY451 was transferred into Δ*aprI* via *E. coli-Streptomyces* conjugation to give WDY451.

HPLC and LC-ESI-HRMS Analysis

Enzymatic reactions and fermentation were monitored by semi-preparative HPLC using a DIONEX System equipped with UltiMate 3000 Pump connecting with Evaporative Light Scattering Detector (ELSD, Alltech 2000ES) and an Diamonsil C18 column (5 μm, 250×4.6 mm). The gas flow and temperature of ELSD was set to 2.9 L/min and 109 °C. Gradient elution was performed at a flow rate of 0.8 mL/min with solvent A (water containing 10mM heptafluorobutyric acid) and solvent B (CH_3CN): 0-3 min, constant 80% A/20% B; 3-5 min, a linear gradient to 75% A/25% B; 5-9 min, a linear gradient to 70% A/30% B; 9-17 min, a linear gradient to 59% A/41% B; 17-18 min, a linear gradient to 80% A/20% B; 18-25 min, constant with 80% A/20% B. LC-ESI-HRMS analysis of samples was performed on a Thermo Electron LTQ-Orbitrap XL fitted with the same column and LC methods. All MS analysis parameters were set as 45 V capillary voltage, 45 °C capillary temperature, auxiliary gas flow rate 10 arbitrary units, sheath gas flow rate 40 arbitrary units, 3.5 kV spray voltage, and 50-1000 Amu mass range.

Isolation and characterization of apramycin intermediates

Compound **3** and **8** was generated Δ*aprI and* Δ*aprI*Δ*aprJ,* respectively. The cells were grown at 37 °C and 220 rpm for 4 days in Minimal medium, and the culture supernatant was collected by centrifugation at 5000 rpm for 30 min. After removal of the insoluble fraction, the supernatant was concentrated and subjected to a semi-preparative HPLC System equipped with Evaporative Light Scattering Detector (ELSD, Alltech 2000ES) and an Agilent ZORBAX SB-C18 column (5 μm, 250×9.4mm). Gradient elution was performed at a flow rate of 3.0 mL/min. The target components eluent was collected and subjected to NMR analysis (Bruker Avance 600-MHz NMR spectrometer).

Protein overexpression and purification

For AprI overexpression, the gene fragment encoding AprI was amplified by PCR from *S. tenebrarius* genomic DNA using primers listed in Table S1. The pET28a (Novagen) vector was digested with *Nde*I/*Hind*III and then ligated with the PCR fragment using Hieff Clone® Plus Multi One Step Cloning Kit (Yeasen, China) to generate pWDY452. The resulting plasmid was confirmed by DNA sequencing and transformed into the *E. coli* BL21(DE3). A single transformant colony was inoculated into LB medium containing 50 mg/L kanamycin and incubated at 37 °C, 220 rpm. 0.2 mM isopropyl IPTG was supplemented to the culture for overexpression induction when OD_{600} reached 0.6 to 0.8. After 16 h incubation at 18 °C, 200 rpm, cell pellet was harvested by centrifugation at 5000 rpm for 10 min, and resuspended in lysis buffer (20 mM Tris-HCl, 300 mM NaCl, 25mM imidazole and 10% (v/v) glycerol, pH 8.0).

The cell suspension was lysed by sonication, and cell debris was removed by centrifugation at 12,000 rpm for 45 min. The supernatant was loaded into Ni-NTA-affinity column twice, and wash by 10 column volumes (CV) of wash buffer (20 mM Tris-HCl, 300 mM NaCl, 25 mM imidazole and 10% (v/v) glycerol, pH 8.0). The target protein was eluted with 5 CV of elution buffer (20 mM Tris-HCl, 300 mM NaCl, 100 mM imidazole and 10% (v/v) glycerol, pH 8.0). 2 mL fractions were collected and subjected to SDS-PAGE analysis. The desired elution fractions were combined and concentrated by centrifugation at 4 °C using an Amicon® Ultra Centrifugal Filters (3 kDa molecular weight cut-off). The concentrated protein solution was subsequently desalted using a PD-10 Column (GE Healthcare) pre-equilibrated with elution buffer (20 mM Tris-HCl, 100 mM NaCl, and 10% (v/v) glycerol, pH 8.0). The resulting purified protein was quantified by NANODROP 2000c (Thermo Scientific) and stored in 10% glycerol at -80 °C until further use.

Enzymatic assays and kinetic characterization of AprI

For the enzymatic assays, a total volume of 100 μL reaction mixture containing 50 mM Tris-HCl (pH 8.0), 1 mM substrate, 2 mM SAM, and 10 μM AprI was incubated at 37 °C for 2 h. Reactions were quenched by adding equal volume of chloroform followed by vigorous vortex and then centrifuged at 13000 rpm for 30 min. The supernatant was subject to HPLC and LC-ESI-HRMS analysis.

A Methyltransferase Activity Assay Kit (Colorimetric) by coupling the methyl transfer reaction to a multi-step enzymatic cascade[3] and resulting in a product which exhibits a strong absorbance at 570 nm was used to perform the kinetic assay for investigating substrate preference of AprI.

The enzyme concentrations for assays using **7** and **8** as substrate are 1 μM and 0.5 μM from pre-experiment, respectively. A mixture of AprI in MT assay buffer, and gradient concentrations (50-4000 μM) of **7** and **8**, was prepared into a series of wells on a 96-well plate. Then the reaction mixture buffer containing 0.5 mM SAM, detection system enzymes and chemicals was added to each well. Absorbance at 570 nm was recorded in kinetic mode every 30 seconds for 30 min at 37 °C using microplate plate reader (Tecan, Infinite 200 PRO). Assays were performed in triplicates.

Agar diffusion assay

Bacillus subtilis was cultured in 5 mL LB medium until OD_{600} reached 0.6. 15 mL LB agar medium was melted and cooled down to 40 °C before mixed with 200 μL of the above culture. The mixture was plated onto a 90 mm petri dish and filter-papers soaked in 5 μL compound solutions (1 mg/mL) were placed onto the solidified agar. The plate was incubated at 37 °C for 12 h before the inhibition zone was evaluated.

Isothermal Titration Calorimetry (ITC) Measurements

The 27-mer RNA oligonucleotide used in ITC experiment was obtained in PAGE-purified grade from TSINGKE Biological Technology (Nanjing, China). The buffer solutions for ITC experiments contained 10 mM sodium cacodylate (pH 5.5), 0.1 mM EDTA, 150 mM NaCl. Thermodynamic data of interaction measurements between RNA oligonucleotide and **1** or **3** were generated using a Malvern MicroCal PEAQ-ITC instrument. Calorimetric titrations were performed with thirteen 3 μL injections with an injection duration of 6 s, a spacing of 150 s, a reference power of 5 μcal/s, and constant temperature at 25 °C. The concentrations used for titration experiments were 2000 μM for compound and 10 μM for RNA oligonucleotide. Data were analyzed with the software provided by the manufacturer, which performed calorimetric binding enthalpy, adsorption constant, number of adsorption sites, and changes in entropy calculations.

Molecular docking

Molecular docking of 16S rRNA with **3** was carried out by autodock[4]. The structure of 16S rRNA nucleosides from apramycin-ribosome complexes structure (PDB entry 4AQY) was used as target macromolecular. Kollman charges and Hydrogens were added to the target macromolecular in AutoDockTools 1.5.7. The energy of ligand was minimized using Chem3D and added Gasteiger charges and Hydrogens in AutoDockTools 1.5.7. The size of the grid box was set to 24,36,46 points in X, Y, Z dimensions, respectively. And the the molecular docking was carried out by AutoDock Vina stand-alone package. The 16S rRNA-3 complex in this study used the docking conformation with the almost lowest binding energy (-7.6).

2. Supplementary Figures

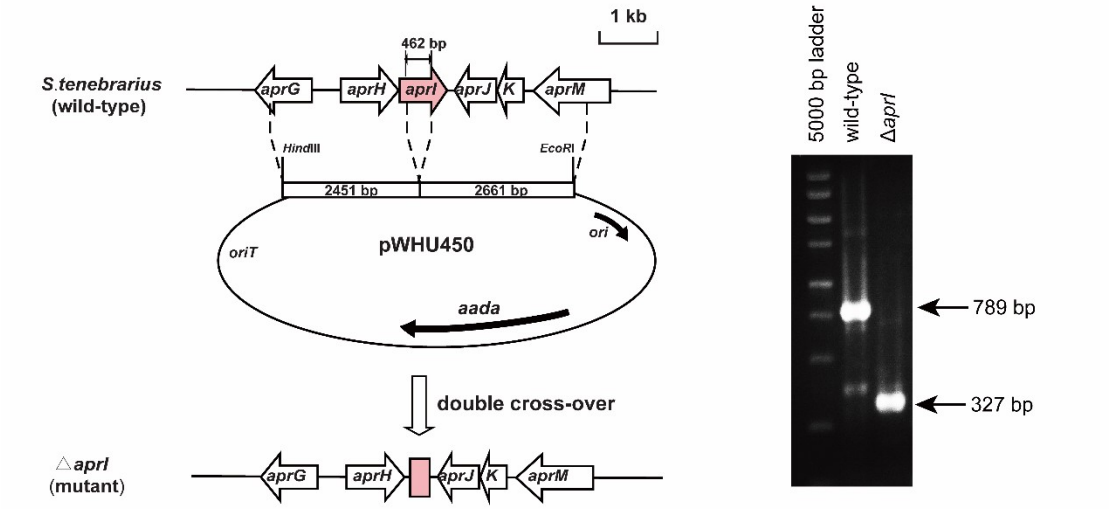

Figure S1. The schematic representation of the in-frame deletion of *aprI* and the PCR verification of Δ*aprI*. The mutant was verified by sequencing with the arrows indicating the expected size of the PCR fragments in the wild-type and mutant. A band at the level of the wild type product in the mutant is the carryover from the wild type lane.

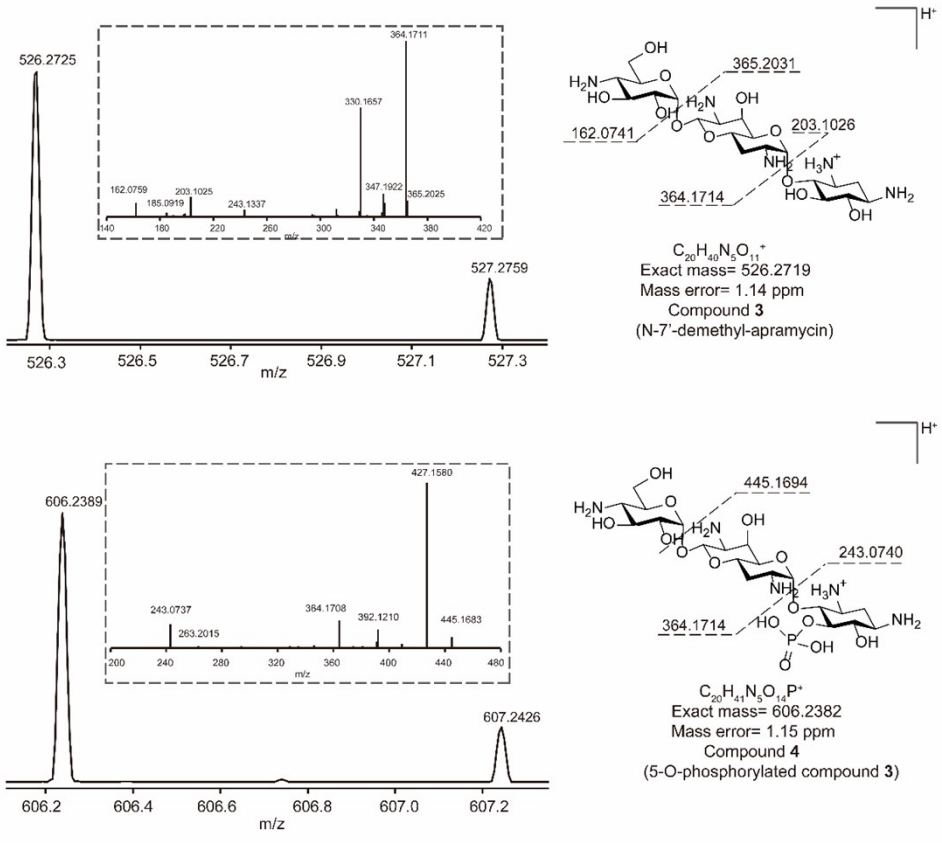

Figure S2. LC-ESI-HRMS and MS/MS analysis of compound 3 and 4. These compounds are detected in positive ion mode and their ion fragments upon collision induced dissociation (CID).

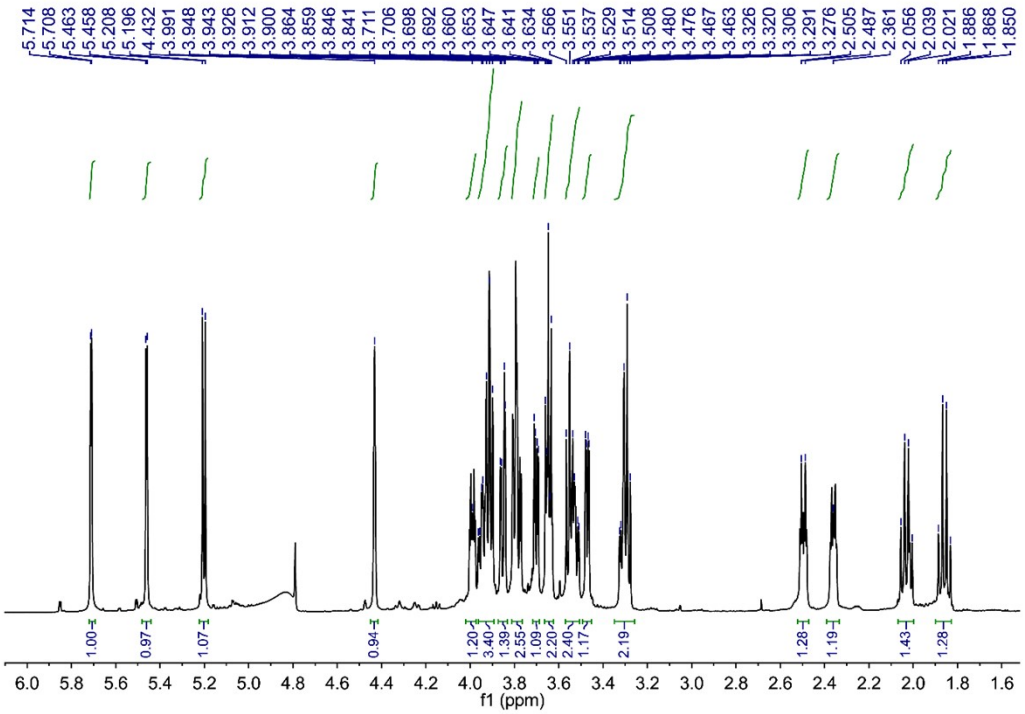

Figure S3. [1]H-NMR sspectrum of compound **3,** which was purified from the fermentation culture of the Δ*aprI* mutant.

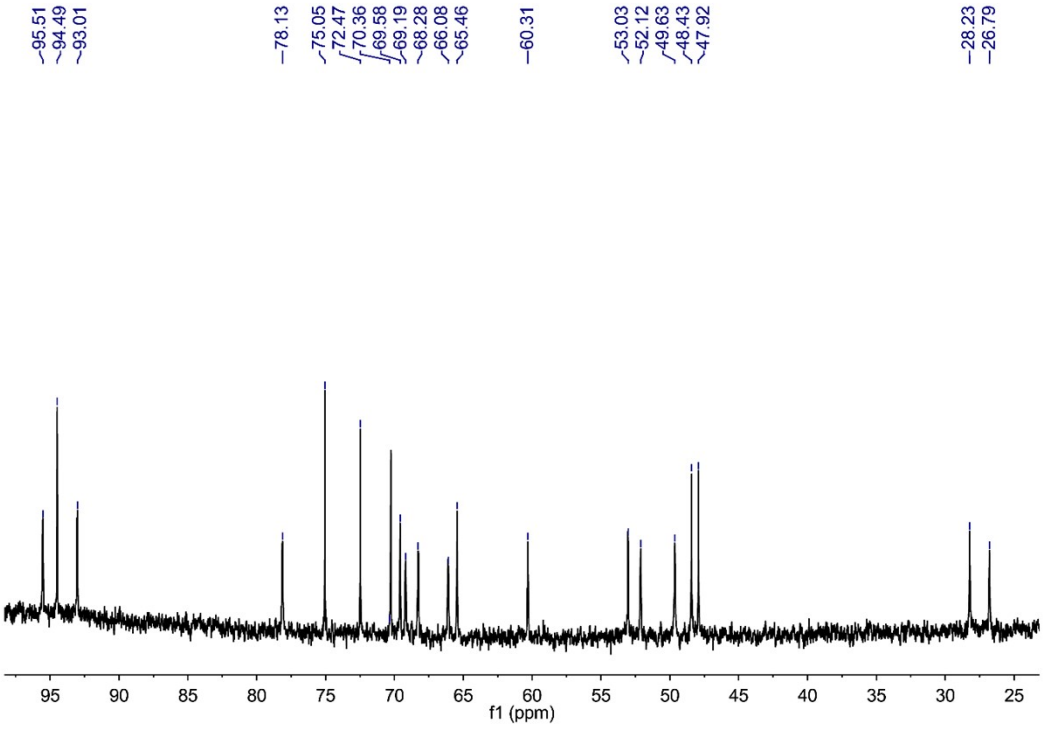

Figure S4. [13]C-NMR spectrum of compound **3,** which was purified from the fermentation culture of the Δ*aprI* mutant.

.

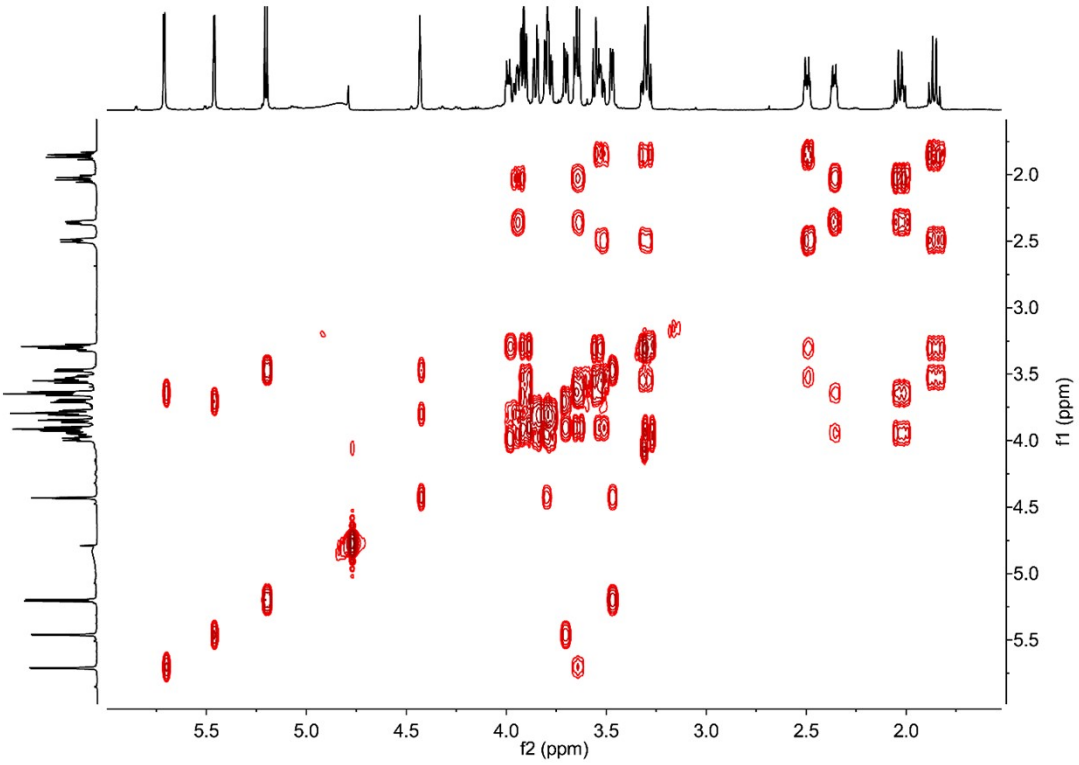

Figure S5. ^{1}H-^{1}H COSY spectrum of compound **3**, which was purified from the fermentation culture of the Δ*aprI* mutant.

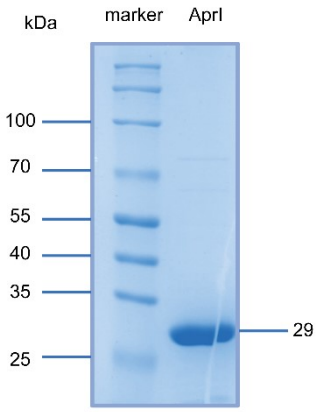

Figure S6. SDS-PAGE analysis of purified AprI.

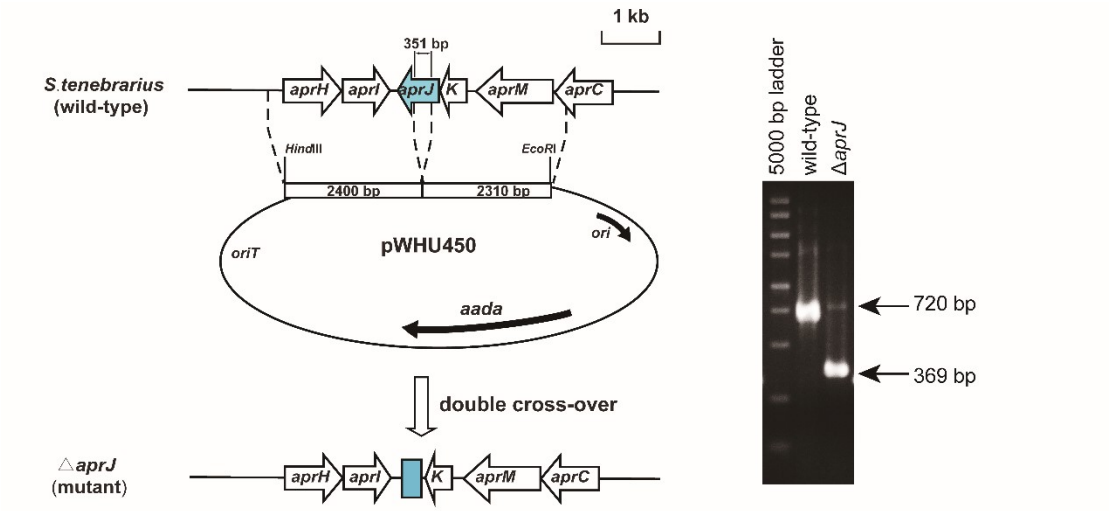

Figure S7. The schematic representation of the in-frame deletion of *aprJ* and the PCR verification of Δ*aprJ*. The mutant was verified by sequencing with the arrows indicating the expected size of the PCR fragments in the wild-type and mutant. A band at the level of the wild type product in the mutant is the carryover from the wild type lane.

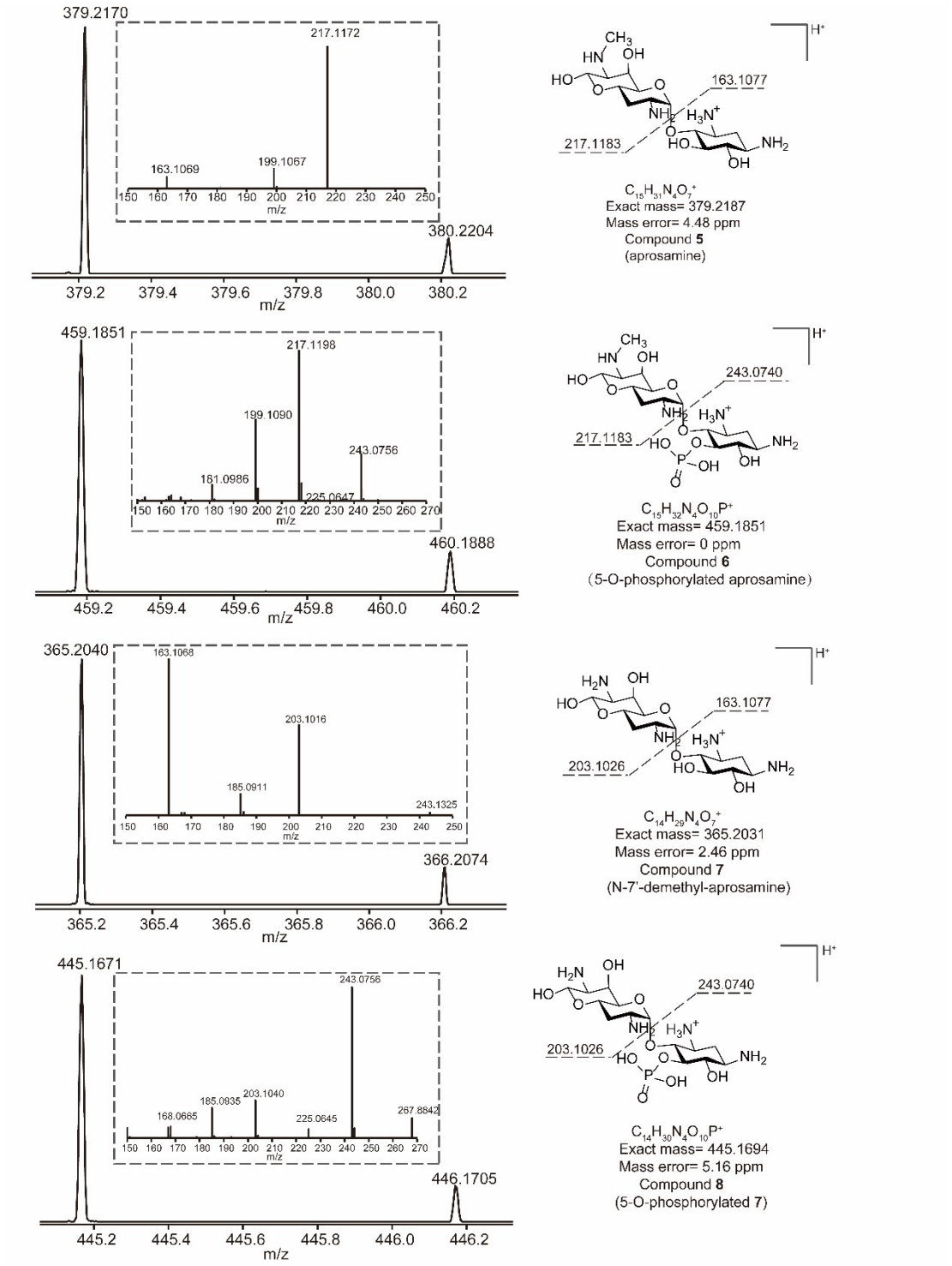

Figure S8. LC-ESI-HRMS and MS/MS analysis of compound **5**, **6**, **7** and **8**. These compounds are detected in positive ion mode and their ion fragments upon collision induced dissociation (CID).

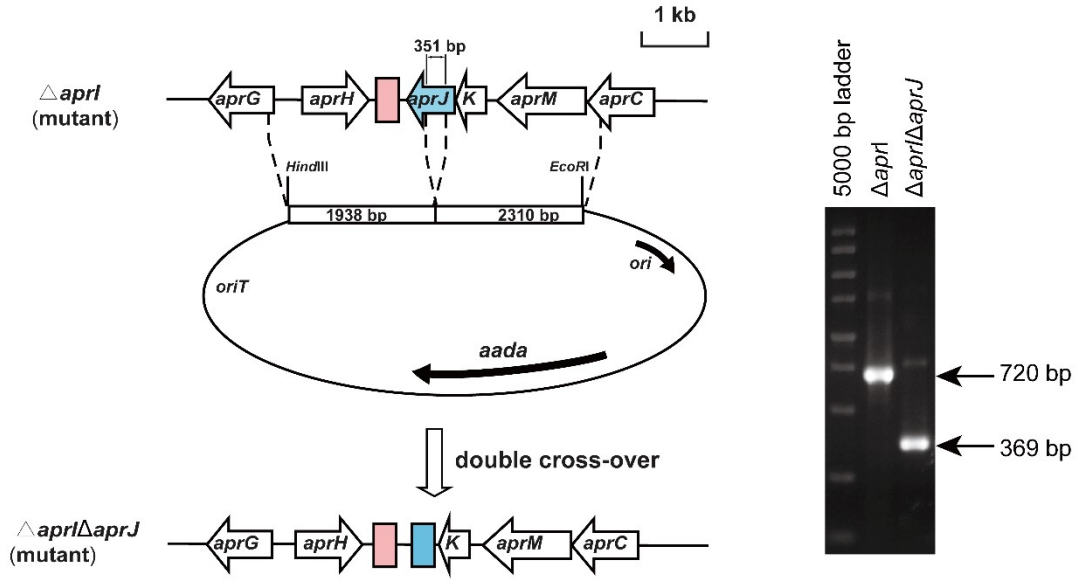

Figure S9. The schematic representation of the in-frame deletion of *aprJ based on* Δ*aprI* and the PCR verification of the double mutant Δ*aprI*Δ*aprJ*. The mutant was verified by sequencing with the arrows indicating the expected size of the PCR fragments in Δ*aprI* and Δ*aprI*Δ*aprJ*. A band at the level of the Δ*aprI* product in the mutant is the carryover from the Δ*aprI* lane.

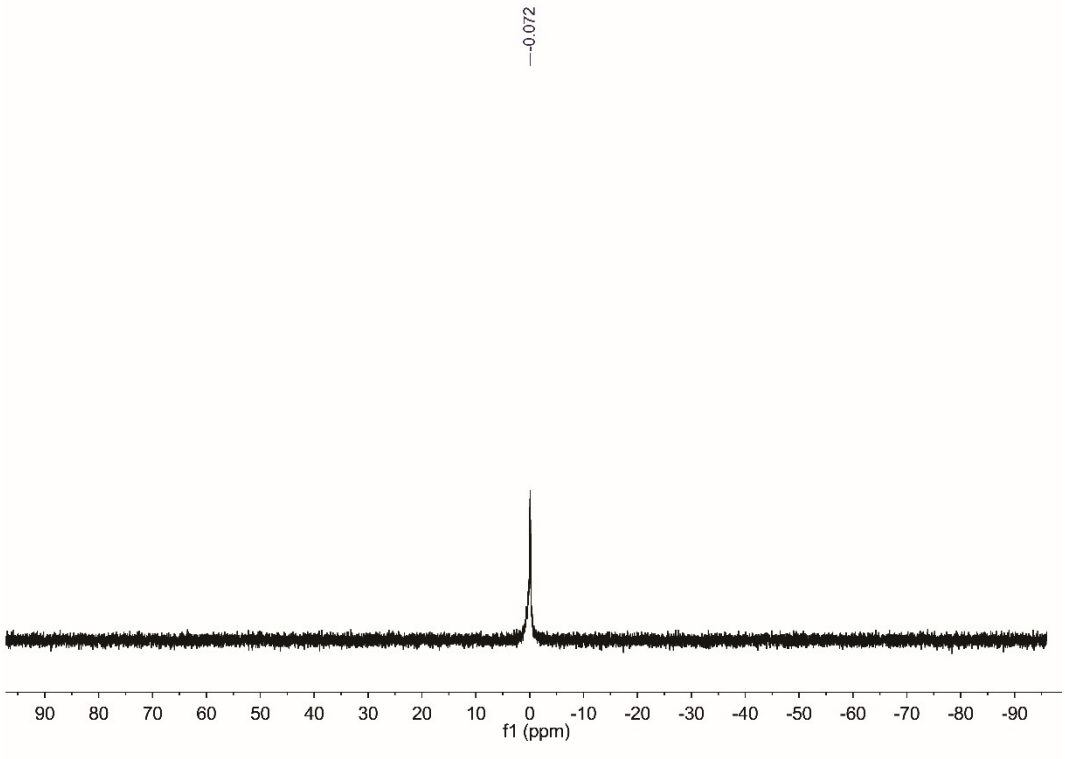

Figure S10. ^{31}P-NMR sspectrum of compound **8**, which was purified from the fermentation culture of the Δ*aprI*Δ*aprJ* mutant.

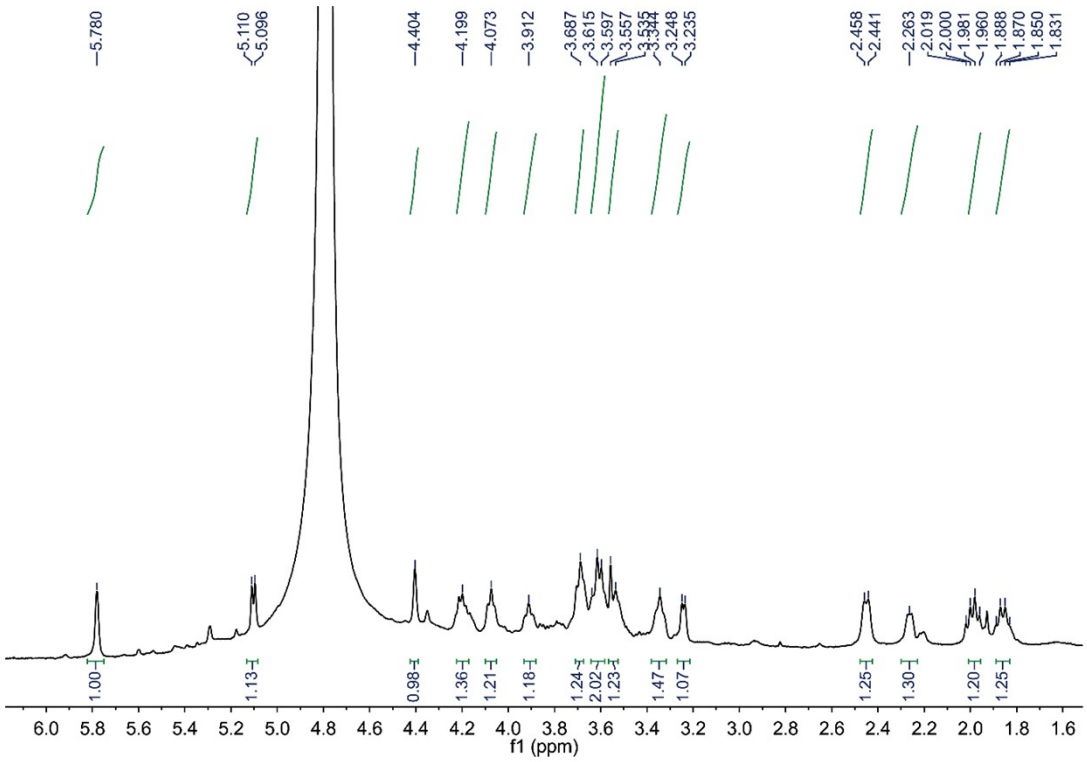

Figure S11. [1]H-NMR sspectrum of compound **8**, which was purified from the fermentation culture of the Δ*aprl*Δ*aprJ* mutant.

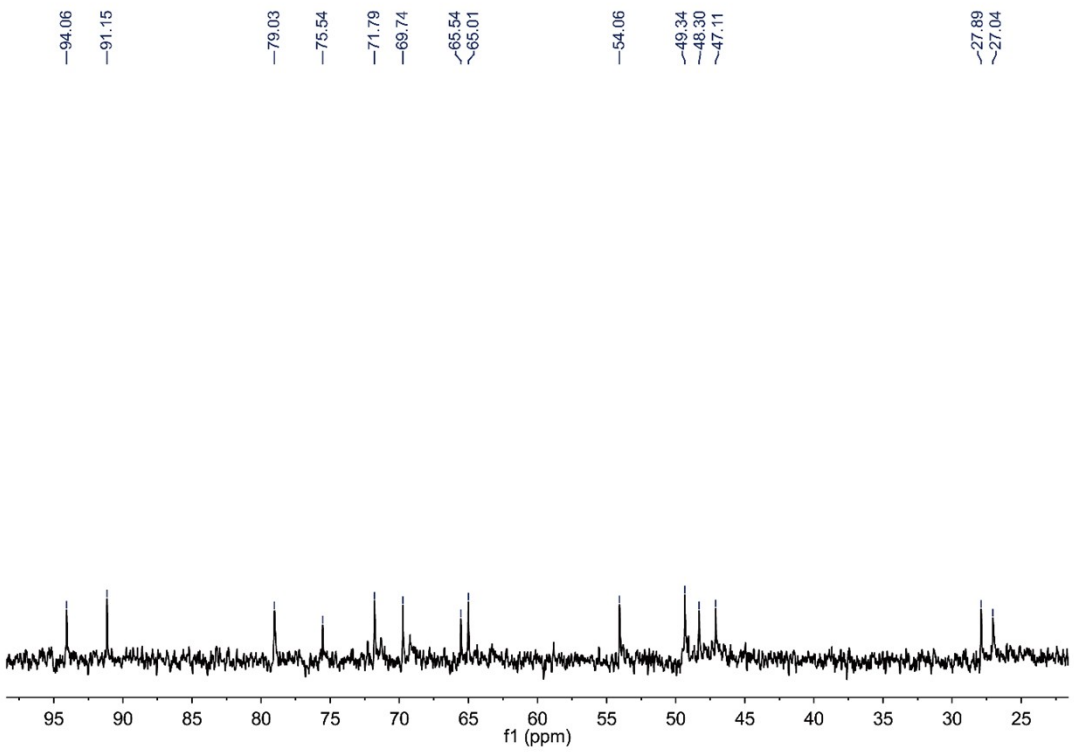

Figure S12. [13]C-NMR spectrum of compound **8**, which was purified from the fermentation culture of the Δ*aprl*Δ*aprJ* mutant.

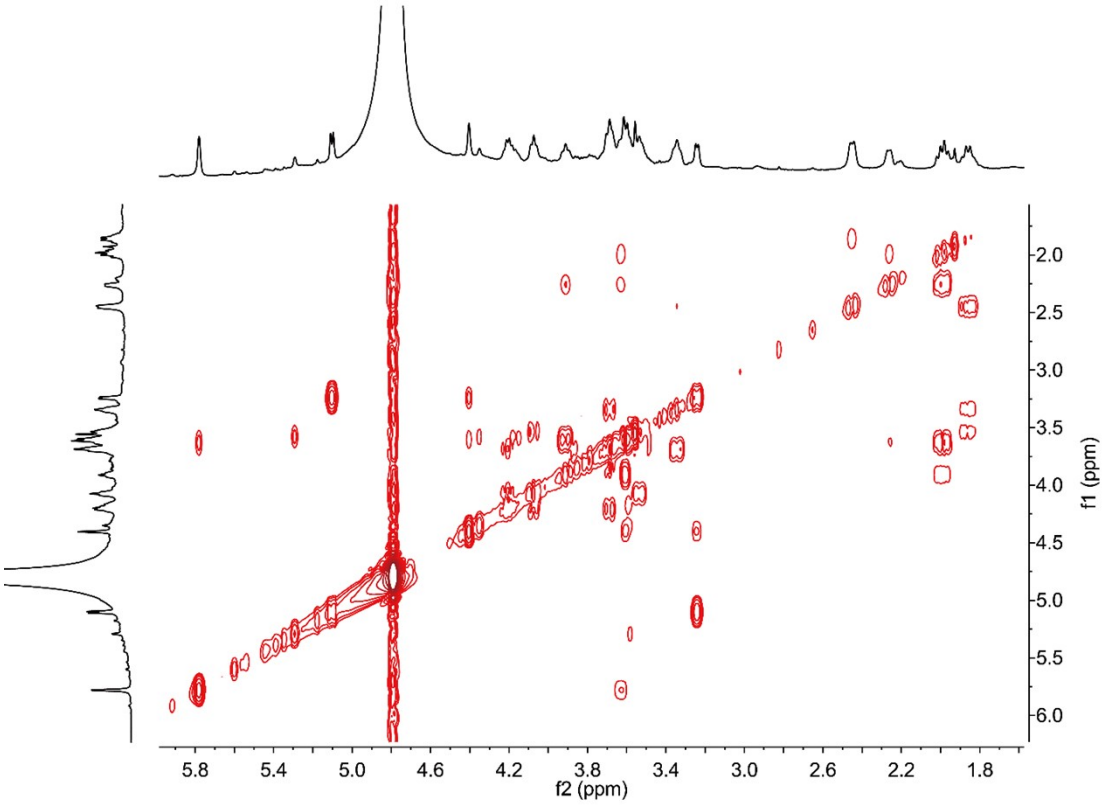

Figure S13. ^{1}H-^{1}H COSY spectrum of compound **8**, which was purified from the fermentation culture of the Δ*aprl*Δ*aprJ* mutant.

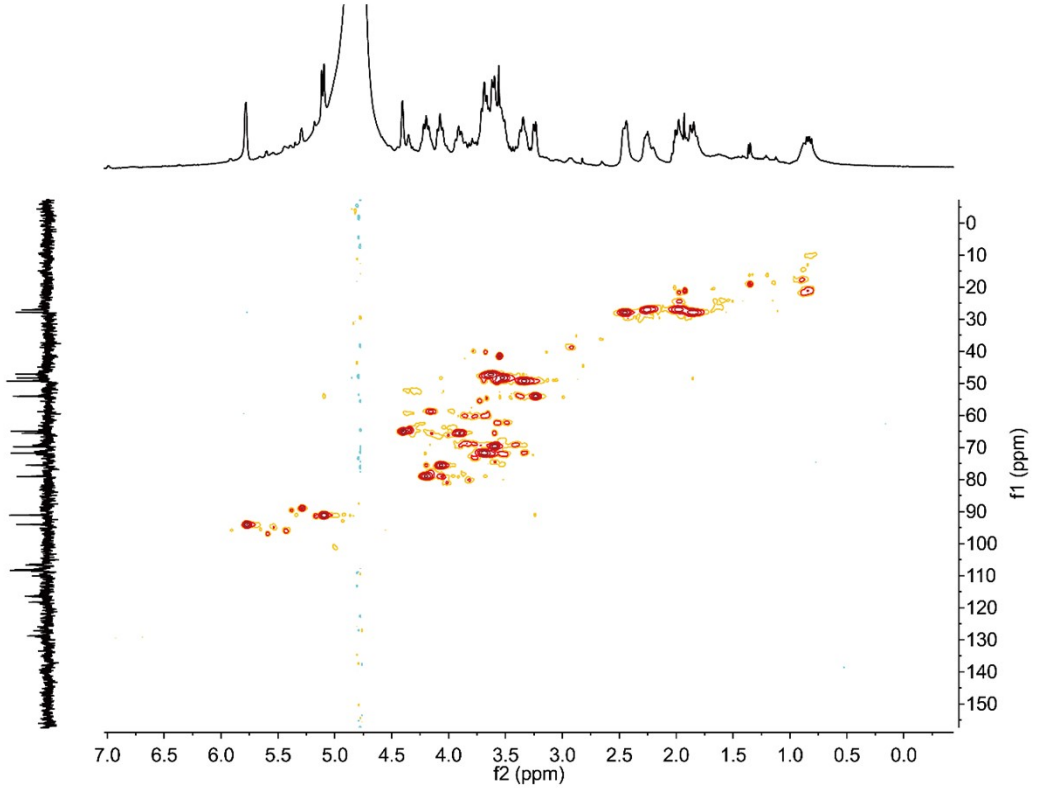

Figure S14. HSQC spectrum of compound **8**, which was purified from the fermentation culture of the Δ*aprl*Δ*aprJ* mutant.

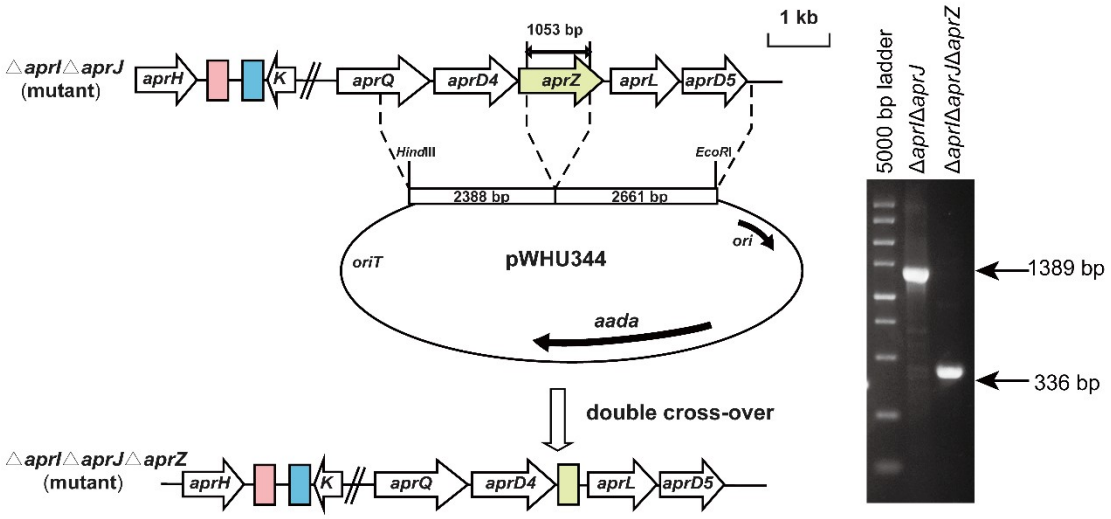

Figure S15. Construction of Δ*aprI*Δ*aprJ*Δ*aprZ* and the PCR verification analysis. The mutant was verified by sequencing with the arrows indicating the expected size of the PCR fragments in Δ*aprI*Δ*aprJ* and Δ*aprI*Δ*aprJ*Δ*aprZ*.

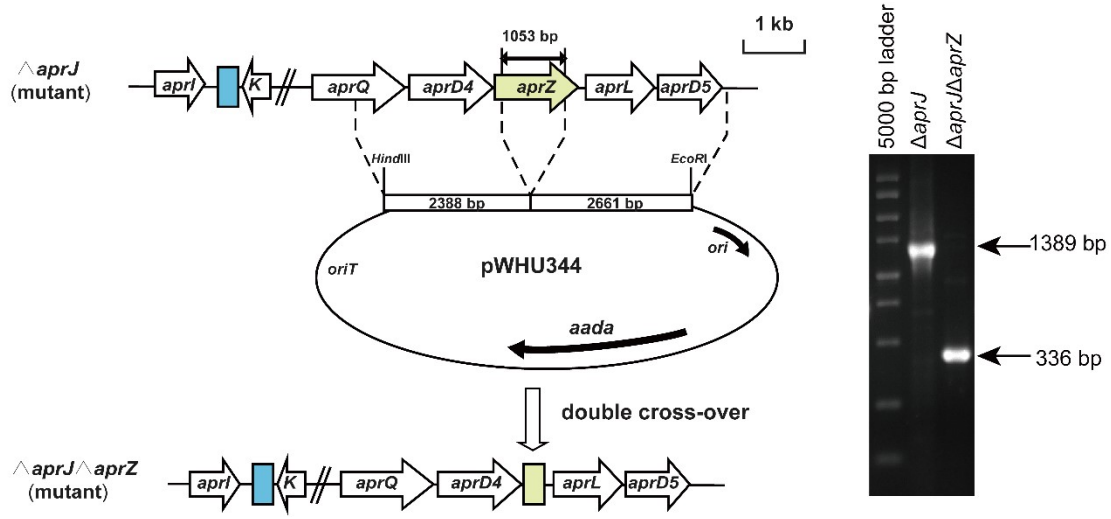

Figure S16. Construction of Δ*aprJ*Δ*aprZ* and the PCR verification analysis. The mutant was verified by sequencing with the arrows indicating the expected size of the PCR fragments in Δ*aprJ* and Δ*aprJ*Δ*aprZ*.

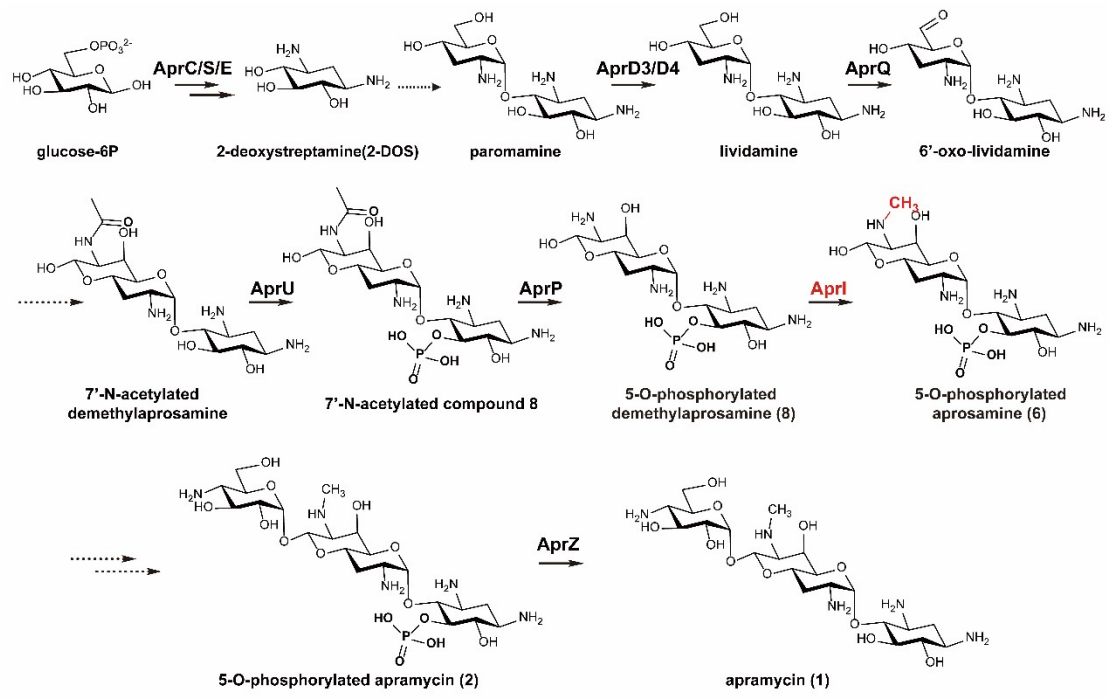

Figure S17. The complete biosynthetic pathway of apramycin. The solid arrows represent the steps that have been elucidated. The uncharacterized steps are shown by dashed arrows.

3. Supplementary Tables

Table S1. Primers used in this study

Primer	Sequence*	Function
aprI-left-F	ACGGCCAGTGCCAAGCTTCGGCGTGGAACACGTTCTTGCGGTCGG	*aprI* in-frame deletion
aprI-left-R	CAGATACAGCCGGCCGAGCACGTACCCGAGCGGGACCCCC	*aprI* in-frame deletion
aprI-right-F	GGCCGGCTGTATCTGGAGATCCCGCTGGAC	*aprI* in-frame deletion
aprI-right-R	TGACATGATTACGAATTCCCCCGGCTGCGGTCGGAGCTGACC	*aprI* in-frame deletion
id-*aprI*-F	GTGCCCAGGATCGACGAGTCCCGCCTGCGC	WDY450 verification
Id-*aprI*-R	TCACTCGTCGGGCCAGGTGAGCTGGTCGAC	WDY450 verification
HB-*aprI*-F	GTAGGATCCACATATGGTGCCCAGGATCGACGAGTCCCG	Δ*aprI* complementation
HB-*aprI*-R	ACATGATTACGAATTCTCACTCGTCGGGCCAGGTGAGC	Δ*aprI* complementation
aprJ-left-F	GGCCAGTGCCAAGCTTCCGCGGAACAGGATCGCACGGTCAACGGAC	*aprJ* in-frame deletion
aprJ-left-R	GCCCTGGGGATCGCCTCGGGTGTTCTCGCCGGGCAGGAGGTGGGCA	*aprJ* in-frame deletion
aprJ-right-F	GGCGATCCCCAGGGCCGCCGCGGCGCCGAC	*aprJ* in-frame deletion
aprJ-right-R	ACATGATTACGAATTCAACAAGCGCGGCTACCTCAGCGACGCGGGC	*aprJ* in-frame deletion
id-*aprJ*-F	GTGAGCCGCGCGGCCACGGGCGAGGGCACC	WDY340 verification
id-*aprJ*-R	CTACGCGACGGGGAGCCGGAGCCCGCCGGG	WDY340 verification
aprI-pET-F	GCCTGGTGCCGCGCGGCAGCCATATGCCCAGGATCGACGAGTCCC	*aprI* overexpression
aprI-pET-R	GGTGCTCGAGTGCGGCCGCAAGCTTTCACTCGTCGGGCCAGGTGA	*aprI* overexpression

*Restriction sites are underlined.

Table S2. Plasmids and strains used in this study

Plasmids	**Relevant genotype**	**Source/Ref.**
pWHU258	aac(3)IV was replaced by aadA in pOJ260	[1]
pWHU268	aac(3)IV was replaced by aadA in pIB139	[1]
pWHU450	*aprI* in-frame deletion construct	This study
pWDY451	*aprI* complementation construct	This study
pWHU340	*aprJ* in-frame deletion construct	This study
pWHU344	aprZ in-frame deletion construct	[2]
pWDY452	*AprI* overexpression construct	This study
Strains	**Relevant comments**	**Source/Red.**
WDY450	*aprI* in-frame deletion mutant	This study
WDY340	*aprJ* in-frame deletion mutant	This study
WDY454	*aprI aprJ* double in-frame deletion mutant	This study
WDY345	*aprJ aprZ* double in-frame deletion mutant	This study
WDY346	*aprI aprJ aprZ* triple in-frame deletion mutant	This study
WDY451	*aprI* complementation mutant	This study
WDY452	BL21(DE3) harboring pWDY452	This study

Table S3. ^{1}H and ^{13}C NMR data of compound 3 and compound 8. ^{1}H (600 MHz) and ^{13}C (150 MHz) NMR spectroscopic data for compound **3** and compound **8** in D_2O.

	Compound 3		**Compound 8**	
position	**δC**	**δH (*mult*, *J*[Hz])**	**δC**	**δH (*mult*, *J*[Hz])**
1	49.63	3.31(m)	49.34	3.34 (m)
2	28.23	a 1.86 (q, *J* = 12.6)	27.89	a 1.84 (m)
		e 2.50 (m)		e 2.45 (d, *J* = 12)
3	48.43	3.54 (m)	48.30	3.54 (d, *J* = 13.2)
4	78.13	3.90 (m)	75.54	4.07 (m)
5	75.05	3.65 (t, *J* = 9.1)	79.03	4.20 (m)
6	72.47	3.55 (t, *J* = 10.5)	71.79	3.69 (m)
1’	95.91	5.71 (d, *J* = 4.2)	94.06	5.78 (s)
2’	47.92	3.64 (m)	47.11	3.62 (m)
3’	26.79	a 2.03 (q, *J* = 11.9)	27.04	a 1.98 (m)
		e 2.36(m)		e 2.26 (m)
4’	66.08	3.95 (m)	65.54	3.91 (m)
5’	69.58	3.80 (m)	69.74	3.60 (m)
6’	65.46	4.43 (t, *J* = 2.1)	65.01	4.40 (s)
7’	53.03	3.47 (dd, *J* = 9.1, 2.8)	54.06	3.25 (d, *J* = 7.8)
8’	93.01	5.20 (d, *J* = 8.4)	91.15	5.10 (d, *J* = 8.4)
1’’	94.49	5.46 (d, *J* = 3.5)	/	/
2’’	70.36	3.70 (dd, *J* = 9.8, 3.5)	/	/
3’’	68.28	3.91 (t, *J* = 9.6)	/	/
4’’	52.12	3.29 (t, *J* = 10.5)	/	/
5’’	69.19	3.99 (m)	/	/
6’’	60.31	3.85(dd, *J* = 12.6, 3.5)	/	/
		3.80(m)	/	/

4. Supplementary References

1. M. Lv, X. Ji, J. Zhao, Y. Li, C. Zhang, L. Su, W. Ding, Z. Deng, Y. Yu and Q. Zhang, Characterization of a C3 Deoxygenation Pathway Reveals a Key Branch Point in Aminoglycoside Biosynthesis, *J Am Chem Soc*, 2016, **138**, 6427-6435.
2. Q. Zhang, H. T. Chi, L. Wu, Z. Deng and Y. Yu, Two Cryptic Self-Resistance Mechanisms in *Streptomyces tenebrarius* Reveal Insights into the Biosynthesis of Apramycin, *Angew Chem Int Ed Engl*, 2021, **60**, 8990-8996.
3. K. M. Dorgan, W. L. Wooderchak, D. P. Wynn, E. L. Karschner, J. F. Alfaro, Y. Cui, Z. S. Zhou and J. M. Hevel, An enzyme-coupled continuous spectrophotometric assay for S-adenosylmethionine-dependent methyltransferases, *Anal Biochem*, 2006, **350**, 249-255.
4. S. Forli, R. Huey, M. E. Pique, M. F. Sanner, D. S. Goodsell and A. J. Olson, Computational protein-ligand docking and virtual drug screening with the AutoDock suite, *Nat Protoc*, 2016, **11**, 905-919.